

CoMFA-SIMCA Model for Antichagasic Nitrofurazone Derivatives

Victor Martinez-Merino^{a,*} and Hugo Cerecetto^b

^aDepartamento de Química Aplicada, Universidad Pública de Navarra, 31006 Pamplona, Spain

^bDepartamento de Química Orgánica, Facultad de Química, Universidad de la República, 11800 Montevideo, Uruguay

Received 18 September 2000; accepted 23 November 2000

Abstract—The physico-chemical properties of some 5-nitro-2-furaldehyde semicarbazones (nitrofurazones) and thiophene analogues were compared with their in vitro and in vivo trypanocidal activity against *Trypanosoma cruzi* (Tulahuen strain). 3D-QSAR models were obtained by applying the SIMCA methodology to the electrostatic and steric fields (CoMFA fields) of the molecules. Nitrofurazones bearing N^4 substituents, which cover a range of 14–17 Å from the nitro group with a thickness of about 6 Å when considering the extended conformer, produced complete survival in infected mice. The in vitro model allows larger N^4 substituents than the *SURVival* model, but they must not bear positive centres in the region 15–16 Å from the nitro group. Moreover, the in vitro model is in agreement with the active site of trypanothione reductase (TR). Both models can be of use in the design of novel drugs bearing an amide-like group at a distance of 7–9 Å from an easily reducible group. © 2001 Elsevier Science Ltd. All rights reserved.

Introduction

Trypanosomiasis is one of the major third-world diseases, with several millions of new infections confirmed annually. *Trypanosoma cruzi* is the etiologic agent of Chagas' disease.^{1,2} The current chemotherapy against this disease is still inadequate and therefore efforts to find antichagasic drugs are of great importance. Recently, we have focused our attention on the development of new compounds that show trypanocide activity.^{3–7} The discovery of a metabolic difference between the pathogen and the mammalian host⁸ has led to a drive to develop new agents based on the active site of the pathogen enzyme trypanothione reductase (TR).^{9,10} The major problem encountered in the application of modelling studies and quantitative structure–activity relationships is that structurally very similar compounds can give rise to completely different inhibition patterns.¹⁰ The active site of TR is quite large and contains various points of interaction for the natural substrate. To date, the combination of such interactions required to activate the biological response remains unknown.

The main drug in use against Chagas' disease is nifurtimox[®], a 5-nitrofurfural derivative.⁴ Nitrofurazones

(5-nitro-2-furaldehyde semicarbazones) also showed a very interesting trypanocidal activity.¹¹ The N^4 substituents on nitrofurazone and the replacement of the furan ring by thiophene in such compounds notably influence the in vitro response against *T. cruzi* epimastigote forms (Tulahuen strain) and the survival of mice infected with *T. cruzi* (Tulahuen strain).^{11,12} Taking into account the above in vitro and in vivo nitrofurazone data, we present here the first trypanocidal model for these kinds of compounds. The model is the result of a three-dimensional quantitative structure–activity relationship study (3-D QSAR) performed using the comparative molecular field analysis (CoMFA) method.¹³ Compounds were categorised as either active or inactive and a categorical analysis technique, the SIMCA method,¹⁴ was used to investigate the relationships between structure and activity. SIMCA analysis has been applied successfully in several QSAR studies^{15–17} when the target property is a nominal rather than a continuous variable, as is the case in the work described here. Significant differences have been found in the in vitro and *survival* CoMFA-SIMCA models.

The nitrofurans interfere with the disulfide reduction of TR and they are also effective as subversive substrates of TR.^{18,19} The derived CoMFA-SIMCA models were therefore compared with the well-known^{20,21} active site of TR.

*Corresponding author. Fax: +34-948-169606; e-mail: merino@unavarra.es

Results and Discussion

Compounds were built using the MMFF94s^{22,23} force field as implemented within the SYBYL molecular modelling program.²⁴ The MMFF94 Force Field²² was developed as a combined organic/protein force field, one that yielded MM3-like accuracy for small molecules and yet was equally applicable to proteins and other systems of biological importance. Our calculations on the nitrofurazone molecule showed that MMFF94s reproduced very well the geometry of this kind of molecule ($RMS = 0.093 \pm 0.039$ Å when all of the atoms were matched to those of fully optimised nitrofurazone from the B3LYP/3-21G (d) density functional theory method,²⁵ as implemented within the Gaussian²⁶ package). The electrostatic potentials around molecules were calculated from MMFF94 partial atomic charges. It is worth noting that the potential minima of nitrofurazone obtained using the B3LYP/3-21G(d) method were well reproduced on using MMFF94 partial atomic charges, and were even better than the values obtained using ESP partial atomic charges extracted from an MNDO semiempirical calculation within MOPAC.²⁷

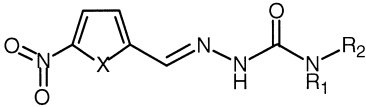
All possible combinations of the CoMFA steric (C_S) and/or electrostatic (C_E) fields, as well as the lipophilicity parameter (R_M),^{28–30} were considered to develop the QSAR models for in vivo survival (a_{SURV}) and in vitro trypanocidal activities (a_{INVIT}) of nitrofurazones against *T. cruzi* (see variables in Table 1). As a consequence, several completely predictive models were obtained (see Table 2). Previous studies support the idea that 5-nitro-furfural derivatives, such as **1–10** and nifurtimox, could act against *T. cruzi* through an intracellular reduction followed by cyclisation to yield a super-oxide

anion.^{4,18,19} However, the reported reduction potentials (E_{pc}) of the 5-nitrofurfural semicarbazones and their corresponding thiophene derivatives, that is **1–18**, vary very little (-0.86 ± 0.01 V and -0.78 ± 0.01 V, respectively)¹² and do not justify the inactivity of the latter compounds. In any case, the E_{pc} data of this series show a standard deviation of less than 10% and so E_{pc} was not considered to be a descriptor variable in these SIMCA analyses.

On using the lattice L_1 and a maximum of four components in the SIMCA analyses on in vivo survival activity, two models based on steric (C_S) or electrostatic and steric ($C_S + C_E$) CoMFA fields gave perfect discrimination between categories (models 1 and 2 for a_{SURV} in Table 2). The model that includes both electrostatic and steric fields (model 2) could be acceptable for the test set of 14 substances (two active). However, complete prediction with a lower number of components (principle of parsimony) occurred when exclusively steric fields (model 1) were taken into account. Model 1 was able to classify correctly all compounds in their categories using one component for the active class and two for the inactive. In contrast, a model including C_S and C_E fields provided the best SIMCA analysis on the in vitro antitrypanosomal activity, where four of the 18 tested compounds showed high activity (model 2 for a_{INVIT} in Table 2). On the other hand, the global lipophilicity of substances within this series seems to be unrelated to the inhibition of Chagas' disease or with the in vitro antitrypanosomal activity.

Figure 1 shows, for *survival* model 1, the steric CoMFA-SIMCA loading contour maps of the first component of active (upper part of Fig. 1) and inactive

Table 1. Dependent and independent variables for the CoMFA-SIMCA analyses

Compound			R_2	a_{INVIT}^a	a_{SURV}^a	R_M^b	I_T^c
	X	R_1					
1	O	H	$-\text{CH}_2(\text{CH}_2)_2\text{CH}_3$	1	1	0.43	0
2	O	H	$-\text{CH}_2(\text{CH}_2)_4\text{CH}_3$	1	0	1.00	0
3	O	H	$-\text{CH}_2\text{CH}_2\text{OCH}_3$	1	1	0.07	0
4	O		$-\text{NR}_1\text{R}_2 = 4\text{-morpholinyl}$	0	0	0.03	0
5	O	H	$-\text{CH}_2\text{CH}_2\text{Ph}$	0	0	0.69	0
6	O	H	$-\text{CH}_2\text{CH}_2\text{-Ph-3,4-OCH}_3$	0	0	0.52	0
7	O	H	$-\text{CH}_2\text{CH}_2\text{CH}_2\text{NHPh}$	1	ND ^d	0.92	0
8	O	H	$-\text{CH}_2\text{CH}_2\text{CH}_2\text{N}(\text{CH}_3)_2$	0	0	0.63	0
9	O	H	$-\text{CH}_2\text{CH}_2\text{CH}_2\text{N}(\text{CH}_2\text{CH}_3)_2$	0	0	0.33	0
10	O	H	$-\text{CH}_2\text{CH}_2\text{CH}_2\text{N}(\text{CH}_2)_5$	0	ND	0.59	0
11	S	H	$-\text{CH}_2(\text{CH}_2)_2\text{CH}_3$	0	0	0.75	1
12	S	H	$-\text{CH}_2(\text{CH}_2)_4\text{CH}_3$	0	0	1.38	1
13	S	H	$-\text{CH}_2\text{CH}_2\text{OCH}_3$	0	0	0.35	1
14	S		$-\text{NR}_1\text{R}_2 = 4\text{-morpholinyl}$	0	0	0.33	1
15	S	H	$-\text{CH}_2\text{CH}_2\text{Ph}$	0	0	1.06	1
16	S	H	$-\text{CH}_2\text{CH}_2\text{-Ph-3,4-OCH}_3$	0	0	0.95	1
17	S	H	$-\text{CH}_2\text{CH}_2\text{CH}_2\text{N}(\text{CH}_3)_2$	0	ND	0.70	1
18	S	H	$-\text{CH}_2\text{CH}_2\text{CH}_2\text{N}(\text{CH}_2)_5$	0	ND	0.72	1

^aCategorised following the Biological data section from refs 12 and 31.

^bRetention parameter from ref 12.

^cPresence of 5-nitrothiophene for lattice L_3 .

^dNo data.

(lower part of Fig. 1) classes. The molecular structures of compounds **7** and **11** are displayed inside the fields as a reference. The steric field maps for \mathbf{a}_{SURV} show that active compounds incorporate N^4 semicarbazone substituents that occupy the zone of space covering a region 14–17 Å from the nitro group with a thickness of about 6 Å (yellow/red contour, upper part of Fig. 1). Negative loadings for the active class in the *survival* model 1 were significant at distances greater than 17 Å from the nitro group and greater than 3 Å from the carbon backbone (purple/white contour, upper part of Fig. 1). The in vitro model 2 shows a region with positive loadings for the active class in $\mathbf{a}_{\text{INVIT}}$ (upper part of Fig. 2) that are slightly bigger than in the \mathbf{a}_{SURV} model (upper part of Fig. 1). This region covers the area 13–18 Å from the nitro group (upper part of Fig. 2). However, unlike \mathbf{a}_{SURV} , the $\mathbf{a}_{\text{INVIT}}$ active class allows N^4 to bear large substituents due to the fact that negative loadings are not intense at a distance 18 Å away from the nitro

group. Furthermore, both bioactivities show negative loadings at distances of about 3 Å surrounding the carbon backbone and at 12–16 Å away from the nitro group (upper part of Figs 1 and 2). On the other hand, loadings around the N^1 substituents are similar for both the \mathbf{a}_{SURV} and $\mathbf{a}_{\text{INVIT}}$ model 2, and reflect to some extent the steric differences between furan and thiophene rings. Furthermore, the discriminating power of the steric field in the region next to the heterocyclic ring in the above SIMCA analyses was poor.

The loadings of the electrostatic CoMFA fields for the $\mathbf{a}_{\text{INVIT}}$ model 2 are shown in Figure 3. Negative loadings surrounding the heteroatom side of the ring in the

Table 2. CoMFA-SIMCA complete predictive models for in vivo survival (\mathbf{a}_{SURV}) and in vitro activities ($\mathbf{a}_{\text{INVIT}}$)

Model	Variables[Lat ^a .]	\mathbf{a}_{SURV} ^b	$\mathbf{a}_{\text{INVIT}}$ ^b
1	$C_S[L_1]$	1 (2)	—
2	$C_S[L_1], C_E[L_1]$	1 (3)	2 (3)
3	$C_S[L_2], C_E[L_2], I_T$	1 (3)	—
4	$C_S[L_2], I_T$	1 (3)	—
5	$C_S[L_2], C_S[L_3]$	1 (3)	—
6	$C_S[L_2], C_E[L_3]$	1 (3)	—

^aLattices L_1 , L_2 and L_3 (see the final section).

^bMinimum number of components for active (inactive) compounds necessary to obtain a perfect discrimination between categories where possible.

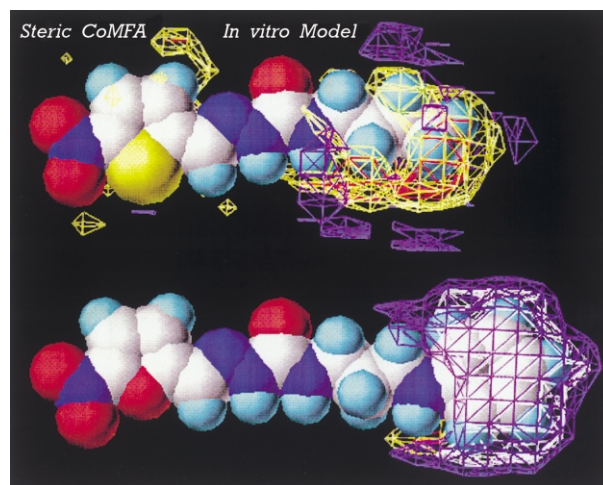


Figure 2. Contour maps of the $\mathbf{a}_{\text{INVIT}}$ steric CoMFA field loadings for the first component of the active (upper) or inactive (lower) class in SIMCA model 2. Contour levels and reference molecules are as in Figure 1.

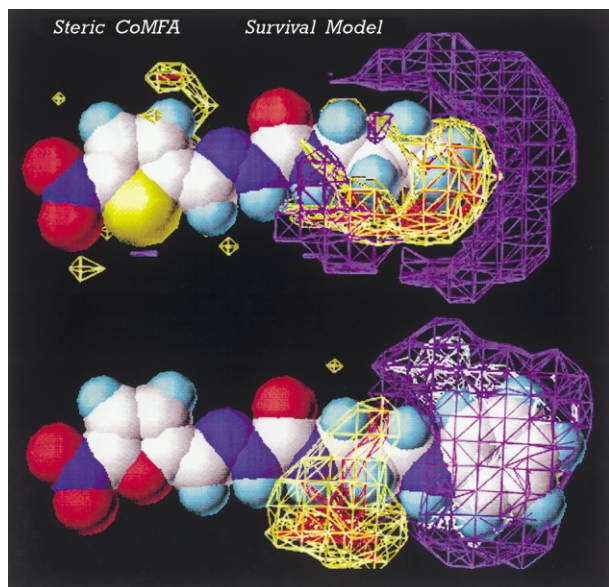


Figure 1. Contour maps of the \mathbf{a}_{SURV} steric CoMFA field loadings for the first component of the active (upper) or inactive (lower) class in SIMCA model 1. Contour levels are -0.06 white, -0.03 purple, 0.03 yellow and 0.06 red. Reference molecules **11** (upper) and **7** (lower) are displayed in space-filling format with the atoms represented by the usual colours.

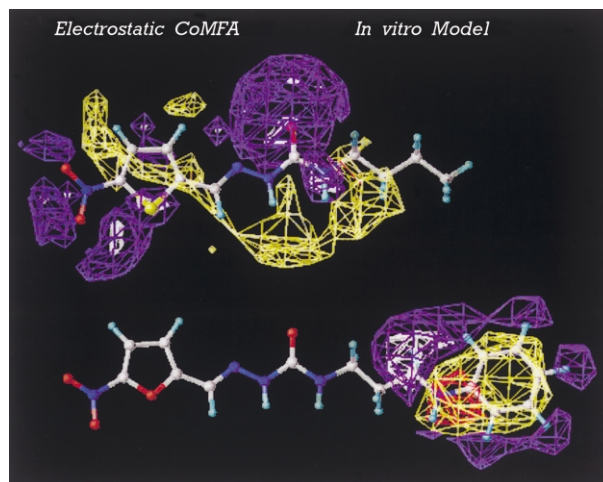


Figure 3. Contour maps of the $\mathbf{a}_{\text{INVIT}}$ electrostatic CoMFA field loadings for the first component of the active (upper) or inactive (lower) class in SIMCA model 2. Contour levels are as in Figure 1. Reference molecules **11** (upper) and **7** (lower) are displayed in ball and stick format with the atoms represented by the usual colours.

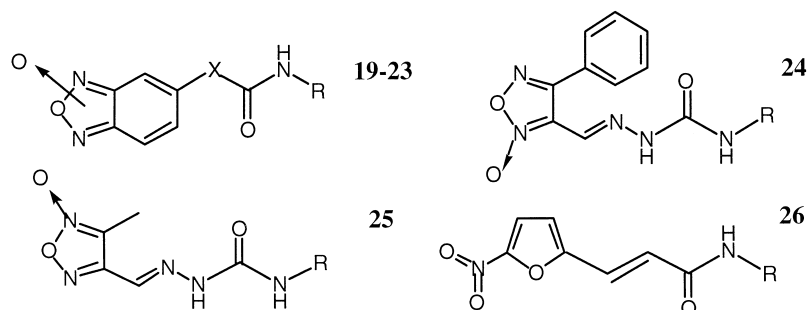
active class seems to be a consequence of significant electrostatic field differences between furan and thiophene. Intense negative fields in this region, as well as around the N^4 atom, could be required to obtain compounds with good trypanocide activity (white contour, upper part of Fig. 3). This observation is in accordance with the discriminating power of the electrostatic field in the SIMCA analysis (data not shown). The loadings in the region occupied by N^4 substituents mainly affect the inactive class (lower part of Fig. 3). Intense negative fields at a distance of about 14 Å from the nitro group decrease the distance to the a_{INVT} inactive class (white contour in the lower part of Fig. 3). Strong positive fields at about 15–16 Å away from the nitro group also diminish the distance to the a_{INVT} inactive class (red contour in the lower part of Fig. 3).

Furthermore, the L_1 region was divided into two other areas (L_2 and L_3) that covered both sides of the semicarbazone substituents (see Experimental). In the L_3 region the compounds only vary from 5-nitrothiophene to 5-nitrofuran and this variation can be described by means of an indicator variable, I_T (Table 1). The analyses performed using the thiophene indicator variable I_T , in conjunction with C_S and C_E , in the L_2 region yielded models with complete discrimination between classes for the in vivo survival bioassays (models 3 and 4 for a_{SURV} in Table 2). These results are similar to those described above for the L_1 region. Variable I_T values could represent any difference between thiophene and furan derivatives, and so equivalent results were obtained when I_T was changed by steric fields (model 5 in Table 2) or electrostatic fields (model 6 in Table 2) in the L_3

region. However, the division of the L_1 region or the introduction of the I_T variable did not give good models for the in vitro activity (all of the completely predictive models needed three or more components for the active class).

The in vitro SIMCA model obtained is in accordance with known data on the active site of trypanothione reductase from the X-ray spectra of the trypanothione-TR complex.²¹ The reactive point in the trypanothione (thiol/disulfide group) is 7–9 Å away from an amide group, which docks the ligand to the enzyme by means of two hydrogen bonds on the GLU-18 and TYR-111 residues. The alkyl chain of this amide group interacts at a distance of 8 Å with a hydrophobic pocket limited by the flat ring of TRP-22 and which also includes the lipophilic part of the TYR-111 and ILE-107 residues. In accordance with these data, the conformational analysis of a nitrofurazone, such as **1**, indicates a separation of 6–9 Å between the oxygen atoms of the carbonyl and nitro groups. The N^4 -butyl substituent in **1**, or even the N^4 -anilinoethyl group in **7**, has the appropriate size to interact with the tryptophan pocket but these two systems need to rotate their carbon backbone to follow the TRP-22 ring, as happens with the spermidine group in the trypanothione ligand. The negative loadings in all SIMCA models near the semicarbazone group are detrimental to the incorporation of rigid N^4 -substituents as rings in this zone, and could be related to the capacity of the N^4 -substituent to be aligned with TRP-22. Similarly, the loadings of the electrostatic CoMFA fields for the inactive class (Fig. 3) seems to be related with a possible interaction between the N^4 -substituent and the TRP-22 residue. On the other hand, the positive loadings for the

Table 3. Percentage of in vitro growth inhibition of *T. cruzi* at a dosage of 25 μM (GI) by some representative compounds and their assignment (a_{PRED}) by the CoMFA-SIMCA model

						
Compound	X	R	GI ^a	a_{INVT}^b	cat0 (cat1) ^c	a_{PRED}
19	-CH=N-NH-	-CH ₂ (CH ₂) ₂ CH ₃	45	0	0.022 (0.022)	0
20	-CH=N-NH-	-CH ₂ (CH ₂) ₄ CH ₃	55	0	0.023 (0.023)	0
21	—	-CH ₂ (CH ₂) ₂ CH ₃	90	1	0.021 (0.022)	0
22	—	-CH ₂ (CH ₂) ₄ CH ₃	79	1	0.023 (0.021)	1
23	—	-CH ₂ CH ₂ CH ₂ N(CH ₃) ₂	15	0	0.022 (0.027)	0
24	—	-CH ₂ (CH ₂) ₄ CH ₃	53	0	0.018 (0.020)	0
25	—	-CH ₂ (CH ₂) ₄ CH ₃	3	0	0.017 (0.020)	0
26	—	-CH ₂ (CH ₂) ₄ CH ₃	100	1	0.019 (0.017)	1

^aFrom refs 4 and 31.

^bCategorised following the Biological data section. The IC₅₀ of the isomeric mixture in the case for **21** and **22** were 10 and 16 μM , respectively. The compound **26** also shows complete growth inhibition at 10 μM .³¹

^cDistances to category 0 (category 1) using the best fit on the reference compound **1**. The 5-substituted derivative was used for **21**, **22** and **23** whereas the 6-derivative was used for **19** and **21**.

steric CoMFA fields in the *survival* model also are in agreement with the structure of the active site of TR. However, it will be necessary to consider other facts in addition to an interaction with TR to explain the inactivity of large nitrofurazones.

Other compounds, such as the recently reported 1,2,5-oxadiazole *N*-oxide derivatives **19–25**, were acceptably classified using the in vitro CoMFA-SIMCA model (see Table 3). Despite the fact that their in vitro activity against *T. cruzi* has been published as being 25 μM ,⁴ the isomeric mixture in the case of **21** and **22** allowed us assign these compounds as being active at 10 μM ($\mathbf{a}_{\text{INVIT}}$ in Table 3). The new nitrofuran derivative **26** was also predicted to be active by this model, and caused complete growth inhibition at 10 μM .³¹

Conclusions

The CoMFA-SIMCA models developed in this work characterise in a precise way the bulk of the semicarbazone *N*⁴-substituents of antichagasic nitrofurazones. The in vitro model describes structural and electronic features that also belong to the pharmacophore of TR, and can be a good guide to obtain new active substances bearing an amide-like group at a distance of 7–9 Å from an easily reducible group. However, in vivo results seem to indicate that nitrofurazones are involved in processes other than interactions with TR. The in vitro test against *T. cruzi* is a good starting point in the search for new lead compounds, but does not show that large *N*⁴ substituents usually produce ineffective antichagasic drugs. Flexible and linear chains bonded to the amide group, which covers a region of 14–17 Å from the reducible group, offers the highest index of survival against *T. cruzi*, as revealed by the *survival* model obtained. The application of the above models as filters in the design of new antichagasic drugs by means of docking analysis, is actually in progress.

Experimental details

Biological data

Eighteen 5-nitro-2-furaldehyde and 5-nitrothiophene-2-carboxaldehyde semicarbazone derivatives were considered in this study (Table 1).

Neither in vivo or in vitro IC_{50} values were available for the compounds. Since, published¹² and personal communication,³¹ the biological data were categorised as:

- For in vivo bioassays compounds were categorised as one (1) when they led to the complete survival of the infected mouse at day 28 of the treatment with a dosage of 66 mg/kg/day from the tenth to the nineteenth day. Otherwise the compounds were categorised as zero (0) (\mathbf{a}_{SURV} , Table 1).
- For in vitro bioactivity, compounds were included in category one (1) when they produced 50% or more growth inhibition of *T. cruzi* at 10 μM , otherwise the compounds were included in category zero (0) ($\mathbf{a}_{\text{INVIT}}$, Table 1).

Calculation of structural properties for QSAR analysis

Firstly the compounds were built with standard bond lengths and angles using the SYBYL 6.6 molecular modelling program.²⁴ The energy of each compound was minimised by molecular mechanics methods using MMFF94s^{22,23} force fields (geometry and charges) with, for the convergence criteria, a gradient of 0.05 kcal/(mol Å). Extended conformers were preferred to calculate the contribution analysis of the backbone substituents on the activity.

The nitrogen of the tertiary amine in compounds **8–10**, **17**, **18** and **23** was considered protonated so the net charge assigned was 1 e.u.; for the rest of the derivatives this value was taken as 0 e.u. The effect of lipophilicity was also investigated. The R_M value of the studied compounds ($R_M = \log [(1/R_f) - 1]$)^{28–30} was introduced as an independent variable into the QSAR analyses (Table 1).¹²

An additional indicator variable (I_T), which describes the presence of 5-nitrothiophene group in the molecule, was also included in some of the QSAR analyses (Tables 1 and 2). This variable could be related with any physico-chemical differences between the two studied nitroheterocycles.

Alignment rule and CoMFA analysis

The alignment rule is the most important input variable in CoMFA. In this study, all molecules were aligned by means of RMS fitting of heavy atoms (C, N and O) of the nitrofurazone moiety, or of its thiophene analogue, using the compound **1** as template molecule. In this alignment, all molecules show a high similarity in the direction of their dipolar moments and in the occupied volume by the residues attached at the *N*⁴- and *N*¹-semicarbazone atoms. Furthermore, semicarbazone and nitro groups could be involved in interactions by means of hydrogen bonds to the receptor, in a similar way to those between trypanothione and the Trypanothione reductase.²¹

A CoMFA lattice \mathbf{L}_1 , with 1 Å of grid spacing, was generated around these molecules based on the molecular volume of the structures. The grid extended beyond the molecular dimensions by 4.0 Å in all directions. The (*x*, *y*, *z*) coordinates of the lowest and highest corners of lattice \mathbf{L}_1 were (−15.40, −7.20, −6.13) and (12.63, 7.81, 5.91), respectively. Two other lattices with 1 Å grid spacings were considered in order to study the *N*⁴- and *N*¹-semicarbazone residues separately. The \mathbf{L}_2 lattice presents corners at (−15.40, −7.20, −6.13) and (1.00, 7.81, 5.91), whereas the \mathbf{L}_3 lattice has corners at (1.00, −7.20, −6.13) and (12.63, 7.81, 5.91). The template molecule was placed in space according to coordinates (−0.51, 0.68, 0.00) and (−0.47, 1.91, −0.02) for the carbon and oxygen atoms of the carbonyl group and (7.54, −1.08, 0.00) for the nitrogen of the nitro group. For the lattices a *Csp*³ was chosen as a probe atom with a charge of +1 and a cut-off of 30 kcal/mol was used for the steric and electrostatic interactions.

The SIMCA algorithm, as implemented within SYBYL,²⁴ derived the 3-D QSAR expression from CoMFA computations. The SIMCA (Soft Independent Modelling by Class Analogy or SIMple Category Analysis) method¹⁴ takes a precategorized training set and, for each category in turn, models the members of that category by the principal components of the explanatory data for that category. The principal components for each category define a hypervolume in which the category members lie. Category membership for a test point then depends upon whether the point falls within one of these defined volumes. In the Tripos implementation of SIMCA,²⁴ which was used by us, the test point is always assigned to one of the predefined categories. A recent study¹⁷ analyses the scope and limitations of this implementation. During the SIMCA analysis, CoMFA-STD was used for scaling and the minimum-sigma value was set to 2.0 kcal/mol in order to minimise the influence of noisy columns. Only in vitro CoMFA-SIMCA models with a maximum number of components of four for the inactive class, which includes 14 cases, and two for the active class (four cases) were considered in the discussion. For the *survival* CoMFA-SIMCA analyses, the maximum number of components accepted was four for the inactive class (12 cases) and one for the active class (two cases).

Molecular coordinates and charges (SYBYL mol2 files), and CoMFA regions are available upon request (merino@unavarra.es).

Acknowledgements

We gratefully acknowledge financial support for this project by the UPNA Research Commission, Pamplona, Spain. The autor thanks CSIC (Universidad de la República — Uruguay) for a scholarship to H. C.

References and Notes

1. Brener, Z. *Pharmacol. Therap* **1979**, *7*, 71.
2. Messeder, J. C.; Tinoco, L. W.; Figueroa-Villar, J. D.; Souza, E. M.; Santa Rita, R.; de Castro, S. L. *Bioorg. Med. Chem. Lett.* **1995**, *5*, 3079.
3. Cerecetto, H.; Di Maio, R.; González, M.; Seoane, G. *Heterocycles* **1997**, *45*, 2023.
4. Cerecetto, H.; Di Maio, R.; González, M.; Risso, M.; Saenz, P.; Seoane, G.; Denicola, A.; Peluffo, G.; Quijano, C.; Olea-Azar, C. *J. Med. Chem.* **1999**, *42*, 1941.
5. Di Maio, R.; Cerecetto, H.; Seoane, G.; Ochoa, C.; Arán, V. J.; Pérez, E.; Gómez Barrio, A.; Muelas, S.; Martínez, A. R. *Arzneim. Forsch.* **1999**, *49*, 759.
6. Olea-Azar, C.; Atria, A. M.; Mendizabal, F.; Di Maio, R.; Seoane, G.; Cerecetto, H. *Spectrosc. Lett.* **1998**, *31*, 99.
7. Olea-Azar, C.; Atria, A. M.; Mendizabal, F.; Di Maio, R.; Seoane, G.; Cerecetto, H. *Spectrosc. Lett.* **1998**, *31*, 849.
8. Fairlamb, A. H.; Blackburn, P.; Ulrich, P.; Chait, B. T.; Cerami, A. *Science* **1985**, *227*, 1485.
9. Chan, C.; Yin, H.; Garforth, J.; McKie, J. H.; Jaouhari, R.; Speers, P.; Douglas, K. T.; Rock, P. J.; Yardley, V.; Croft, S. L.; Fairlamb, A. H. *J. Med. Chem.* **1998**, *41*, 148 and references cited therein.
10. Bonse, S.; Santelli-Rouvier, C.; Barbe, J.; Krauth-Siegel, R. L. *J. Med. Chem.* **1999**, *42*, 5448.
11. Cerecetto, H.; Di Maio, R.; Ibarruri, G.; Seoane, G.; Denicola, A.; Peluffo, G.; Quijano, C.; Paulino, M. *Il Farmaco* **1998**, *53*, 89.
12. Cerecetto, H.; Di Maio, R.; González, M.; Risso, M.; Sagrera, G.; Seoane, G.; Denicola, A.; Peluffo, G.; Quijano, C.; Basombrio, M. A.; Stoppani, A. O. M.; Paulino, M.; Olea-Azar, C.; Eur. *J. Med. Chem.* **2000**, *35*, 343.
13. Cramer, R. D., III.; Patterson, D. E.; Bunce, J. D. *J. Am. Chem. Soc.* **1988**, *110*, 5959.
14. Wold, S. *J. Pattern. Recogn.* **1976**, *8*, 127.
15. Droge, J. B. M.; Van't Klooster, H. A. *J. Chemometrics* **1987**, *1*, 221.
16. Dunn, W. J.; Wold, S. J.; Martin, Y. C. *J. Med. Chem.* **1978**, *21*, 922.
17. Hunt, P. A. *J. Comp.-Aided Mol. Des.* **1999**, *13*, 453.
18. Blumenstiel, K.; Schoneck, R.; Yardley, V.; Croft, S. L.; Krauth-Siegel, R. L. *Biochem. Pharmacol.* **1999**, *58*, 1791.
19. Henderson, G. B.; Ulrich, P.; Fairlamb, A. H.; Rosenberg, I.; Pereira, M.; Sela, M.; Cerami, A. *Proc. Natl. Acad. Sci. U.S.A.* **1988**, *85*, 5374.
20. Bond, C. S.; Zhang, Y.; Berriman, M.; Cunningham, M. L.; Fairlamb, A. H.; Hunter, W. N. *Structure Fold Des.* **1999**, *7*, 81.
21. Structure 1BZL (EC: 1.6.4.8, Trypanothione Reductase (oxidized form) complexed with FAD, GCG and water molecules) from <http://www.rcsb.org/pdb>
22. Halgren, T. *J. Am. Chem. Soc.* **1990**, *112*, 4710.
23. Halgren, T. *J. Comp. Chem.* **1999**, *20*, 720 and 730.
24. Sybyl v. 6.6 (1999), Tripos Associates, 1699 South Hanley Road, Suite 303, St. Louis, MO 63144, USA.
25. Becke, A. D. *J. Chem. Phys.* **1993**, *98*, 5648.
26. Frisch, M. J.; Trucks, G. W.; Schlegel, H. B.; Gill, P. M. W.; Johnson, B. G.; Robb, M. A.; Cheeseman, J. R.; Keith, T. A.; Petersson, G. A.; Montgomery, J. A.; Raghavachari, K.; Al-Latham, M. A.; Zakrzewski, V. G.; Ortiz, J. V.; Foresman, J. B.; Cioslowski, J.; Stefanov, B. B.; Nanayakara, A.; Challacombe, M.; Peng, C. Y.; Ayala, P. Y.; Chen, W.; Wong, M. W.; Andrés, J. L.; Replogle, E. S.; Gomperts, R.; Martin, R. L.; Fox, D. J.; Binkley, J. S.; Defrees, D. J.; Baker, J.; Stewart, J. J. P.; Head-Gordon, M.; González, C.; Pople, J. A. *GAUSSIAN 94*, Revision C.3; Gaussian, Inc.: Pittsburgh, PA, 1995.
27. Stewart, J. J. P. *J. Comp.-Aided Mol. Des.* **1990**, *4*, 1.
28. Tsantili-Kakoulidou, A.; Antoniadou-Vyza, A. *J. Chromatogr.* **1988**, *445*, 317.
29. Denny, W. A.; Atwell, G. J.; Roberts, P. B.; Anderson, R. F.; Boyd, M.; Lock, C. J. L.; Wilson, W. R. *J. Med. Chem.* **1992**, *35*, 4832.
30. Chowdhury, H.; Saxena, V. S.; Walia, S. *J. Agric. Food Chem.* **1998**, *46*, 731.
31. Denicola, A.; Peluffo, G.; Quijano, C. Personal communication.